

Borrowed Identities: Malleable Distillation Factories and a Unified Numerical Search

Shraddha Singh,^{1,2,3,*} Craig Gidney,¹ and Cody Jones¹

¹Google Quantum AI

²Department of Applied Physics, Yale University, New Haven, Connecticut 06511, USA

³Yale Quantum Institute, Yale University, New Haven, Connecticut 06511, USA

Magic-state distillation is one of the leading overheads in fault-tolerant quantum computation. Existing methods for finding distillation factories require a transversal gate to act correctly on the entire codespace, a constraint that limits both generality and search efficiency. We introduce a strictly weaker *borrowed-identity* condition, requiring only that the distillation circuit act as the identity on a single input state. It applies uniformly across all levels of the Clifford hierarchy and unifies, within a single level, factories that distill different magic states—for example, the $|T\rangle$, $|\text{CS}\rangle$, and $|\text{CCZ}\rangle$ factories. A brute-force search over borrowed-identity circuits with two-group symmetry recovers, within the search range, all distance-2 factories known from code-construction approaches, including entangled-output and multi-output factories previously outside the scope of any single numerical search. This unification yields parent circuits that encode multiple factories, so the output magic-state type can be chosen at compile time rather than fixed by a hard-coded design. The framework also extends beyond CSS codes, unifying constructions, including synthillation and non-CSS catalytic factories, previously obtained by disparate approaches.

Fault-tolerant quantum computation (FTQC) requires a universal gate set, the Clifford group with a non-Clifford gate [1]. Yet, most practical quantum error-correcting codes admit a constant-depth fault-tolerant implementation only for the Clifford group [2]. The standard route to universality is gate teleportation [3]: a non-Clifford gate U is applied by consuming a magic state $|U\rangle$. For the $T = e^{-i\pi Z/8}$ gate, the relevant resource is $|T\rangle = T|+\rangle = |0\rangle + e^{i\pi/4}|1\rangle$ (unnormalized). Magic-state distillation (MSD) [1, 4] purifies many low-fidelity logical copies of this state into fewer high-fidelity ones using only Clifford operations, with overhead

$$O(\log^\gamma(1/\epsilon)), \quad \gamma = \log_d\left(\frac{N}{k}\right), \quad (1)$$

where N inputs yield k outputs at distance d and target error rate ϵ . Low γ is a desirable property for reducing FTQC overhead. MSD remains a crucial component in projected fault-tolerant architectures [5–7].

Prior constructions of distillation factories with practically relevant $[[N, k, d]]$ parameters broadly operate in the *Heisenberg picture*, demanding that a transversal gate act correctly on every logical state, the constraint of triorthogonality and quasitransversality, and making the corresponding searches non-linear matrix problems [8–15], barring some limited exceptions [16, 17]. A complementary perspective on distillation was offered by Litinski [18], who observed that the factories $[[15, 1, 3]]$, $[[14, 2, 2]]$, and $[[20, 4, 2]]$ can be represented via spacetime dual of the respective transversal implementation on CSS codes with a common circuit structure: they are all derived from identity circuits on $|+\rangle^{\otimes n}$ built from multi-qubit Z -rotations. These circuit examples were not given an algebraic formulation and no systematic search was built on it.

In this Letter, we formalize this observation of Ref. [18] as a *borrowed-identity condition* in the Schrödinger picture, asking only that the circuit act as identity on a

specific input state through the collective phase action of its gates, with no requirement that it act as identity on the full codespace – the identity is borrowed from the input state. A distillation factory is then obtained from a borrowed identity on n qubits using N gates by removing all gates acting solely on k qubits: the k affected qubits are left in a desired magic state $|\theta\rangle$ and serve as distilled outputs, while the remaining $n - k$ qubits are measured in the X basis for error detection. A note on conventions: we use n for the circuit’s qubit count and N for its gate count, which become the number of X -stabilizers and input magic states, respectively, in the spacetime-dual CSS code. Most of the distillation literature uses n for our N . Under the spacetime rotation that exchanges qubits with stabilizer ancillae and phase rotations with magic-state inputs, the n -qubit borrowed identity built from N multi-qubit Z -rotations becomes an N -qubit CSS code with n X -stabilizer measurements on which $T^{\otimes N}$ acts as a logical Clifford-hierarchy gate. The borrowed-identity condition $\mathcal{C}|+\rangle^{\otimes n} = e^{i\phi}|+\rangle^{\otimes n}$ corresponds, in the dual picture, to all X -stabilizer measuring ancillae returning to the $|+\rangle$ state.

We derive the conditions under which a borrowed identity serves as a distillation factory; unlike all prior frameworks, they are parameterized by $\theta = \pi/2^l$ and hold at every level l of the Clifford hierarchy without modification: the same algebraic machinery searches for S -gate factories ($l = 2$), T -gate factories ($l = 3$), and higher-level rotation factories ($l \geq 4$) simultaneously. The relaxation has three concrete payoffs. First, a closed-form master equation (Theorem 3) recovers the quantum Reed–Muller code [19] $[[2^{l+1} - 1, 1, 3]]$ analytically at every l . Second, extending the construction to circuits with entangled outputs (like CS and CCZ magic states) recovers the generalized triorthogonal family [10, 20], for example, the hypercube quantum code family $[[2^l, l, 2]]$ [21, 22] such as $[[8, 3, 2]]$

(T -to-CCZ) and $[[16, 4, 2]]$ (T -to-CCCZ); and the T -to-CS factory $[[12, 2, 2]]$ [23] (equivalent to the 4 CS \rightarrow 1 CS factory derived from AG codes [24]), providing the first systematic search over these factories for arbitrary l . A two-group asymmetric circuit yields a phase condition linear over $\mathbb{Z}_{2^{l+1}}$ (Theorem 5), with verification costing $O(k(n-k))$ phase computations, growing only polynomially in n and k . Third, we show malleable circuits for arbitrary l that unify factories distilling different magic states at the same Clifford-hierarchy level (for example, the T -to- T , T -to-CS, and T -to-CCZ factories at $l = 3$).

An unoptimized brute-force Python implementation on the asymmetric circuit search conditions, run on a standard laptop (Apple M4, 16 GB RAM), recovers in ~ 9 seconds every distance-2 factory within the swept range $l \in \{2, 3, 4\}$, $k \leq 7$, $n \leq 11$, and gate-weight parameters $s_{\text{total}}, s_O \leq 7$ (21,920 valid factories in total) [25]. Unlike traditional distillation conditions parametrized by N , our search is parametrized by n , which stays small even for $[[N, k, d]]$ factories with large N . The result includes well-known factories that no prior single framework captures simultaneously: the H-code $[[k+4, k, 2]]$ family ($l = 2$), the Bravyi-Haah $[[3k+8, k, 2]]$ family ($l = 3$), all distance-2 entries of the Nezami-Haah triorthogonal-code catalogue [26] at the largest k for each N , and the small distance-2 AG-codes [24] (see Fig. 1). The $k \leq 7$ ceiling is a property of the swept range and not of the framework: since the runtime scales only polynomially in n and k , any distance-2 factory at larger k is reachable by widening the sweep.

Framework— For $\theta = \pi/2^l$, $l \in \mathbb{Z}_{\geq 1}$, the *magic state* is $|\theta\rangle := |0\rangle + e^{i2\theta}|1\rangle$ (unnormalized). The weight- w phase rotations to be used in the circuit are

$$Z^{\otimes w}(\theta) := \exp\left(i\theta\left(I - \bigotimes_{j=1}^w Z_j\right)\right), \quad (2)$$

which apply phase $e^{i2\theta}$ to basis states with an odd number of 1s among the w designated qubits. The gates $Z^{\otimes w}(\pi/2^l)$ are diagonal elements of the l -th level of the Clifford hierarchy \mathbb{C}_l [3], and the diagonal subgroup of \mathbb{C}_l is closed under products [27].

Definition 1 (Borrowed identity). A circuit \mathcal{C} on n qubits, built from parity phase gates with $\theta = \pi/2^l$, is a *borrowed identity* if $\mathcal{C}|+\rangle^{\otimes n} = e^{i\phi}|+\rangle^{\otimes n}$ for some global phase ϕ . This framework formalizes the construction of Ref. [18] to re-envision distillation factories in the Schrödinger picture, where only the state of the qubits is tracked, unlike the Heisenberg picture (see App. A), where the transversality of an operation is tracked. Because this circuit is built entirely from gates in the diagonal \mathbb{C}_l subgroup, the k -qubit output state of the factory, obtained by removing gates from the borrowed identity which act solely on the output qubits, is necessarily a resource state that

teleports a diagonal \mathbb{C}_l gate using conditional operations from \mathbb{C}_{l-1} . A distance-2 factory is guaranteed with such a borrowed identity construction since all phase rotations have dependency on a non-output (check) qubit which will detect any single error in the circuit upon measurement in the X basis.

Our framework changes the search from generalized tri-orthogonal codes to borrowed-identity circuits, treated below in three settings: symmetric (closed-form conditions), two-group (brute-force search), and malleable circuits.

a. Symmetric circuits— When a circuit is invariant under the full symmetric group S_n on the n qubits [28], the gate set is specified by allowed weights $\mathcal{W} \subseteq \{1, \dots, n\}$ with all $\binom{n}{w}$ gates of each $w \in \mathcal{W}$ included. States of equal Hamming weight i accumulate identical phase, so it suffices to track the Dicke sector $|\binom{n}{i}\rangle := \sum_{|\mathbf{x}|=i} |\mathbf{x}\rangle$.

Lemma 2 (Dicke-sector phase accumulation). *For the above symmetric circuit, every element of $|\binom{n}{i}\rangle$ accumulates the total phase*

$$\Phi(i) \equiv 2^i \theta \sum_{\substack{w \in \mathcal{W} \\ w \geq i}} \binom{n-i}{w-i} \pmod{2\pi}. \quad (3)$$

The full inductive proof is given in App. B.

Theorem 3 (Symmetric master condition). *A symmetric circuit with gate set \mathcal{W} and $\binom{n}{w}$ gates of each weight is a borrowed identity if and only if*

$$\sum_{\substack{w \in \mathcal{W} \\ w \geq i}} \binom{n-i}{w-i} \in 2^{l-i+1} \mathbb{Z} \quad \text{for all } i \in \{1, \dots, l\}. \quad (4)$$

For $i > l$, the prefactor in Eq. (3) is $2^i \theta = 2m\pi$ where m is an integer; the condition is satisfied automatically. The distance of the code is determined by the minimum number (d) of gates whose combination has an odd overlap on not more than k qubits.

For $\mathcal{W} = \{w : w \equiv 1 \pmod{s}\}$, increasing s , the weight separation parameter, straightforwardly increases the output qubits to yield $[[N-s, s, 2]]$, for every choice of s , where N is the total number of gates in the borrowed-identity for an admissible \mathcal{W} satisfying Eq. (4). For example, when $s \in \{1, 2\}$, Eq. (4) admits closed-form solutions. Taking $\mathcal{W} = \{1, 2, \dots, n\}$ ($s = 1$) gives $n_{\min} = l + 1$ with $N = 2^{n_{\min}} - 1$ yielding the code parameters $[[2^{l+1} - 2, 1, 2]]$; taking odd weights [29] only ($s = 2$) gives $n_{\min} = l + 2$ while the total number of gates is given by $2^{n_{\min} - 1}$. This circuit allows removing two weight-1 gates from the circuit to yield $[[2^{l+1} - 2, 2, 2]]$, recovering the smallest Bravyi-Haah code $[[14, 2, 2]]$ for $l = 3$ and the smallest H-code $[[6, 2, 2]]$ [17] for $l = 2$ (the $l = 1$ member $[[2, 2, 2]]$ is degenerate; the $[[4, 2, 2]]$ Iceberg code [30] instead appears as the $l = 2$, degree-2 two-group member, see Table V). The

solution for $s = 2$ can be extended to yield $[[2^{l+1} - 1, 1, 3]]$ if we only remove a single weight-1 gate, recovering the Steane code $[[7, 1, 3]]$ [31] at $l = 2$ and the $[[15, 1, 3]]$ distillation factory [1] at $l = 3$. Factories with $s \geq 3$ have no closed-form solution and require numerical search ($k \geq 3$, $d = 2$ fall here); increasing s does not raise the distance, which saturates at $d = 3$ (App. B). The $s = 2$ result thus gives distance-3 distillation at every Clifford level—the quantum Reed–Muller family [19], here derived without reference to any codespace [32–34]. The more efficient entangled-output and higher-rate factories, however, require relaxing the full S_n symmetry.

b. Two-group symmetric circuits— To simplify search on asymmetric circuits, we partition the n qubits into k output qubits (\mathcal{O}) and $n - k$ check qubits (\mathcal{S}), keeping qubits within each group interchangeable ($S_k \times S_{n-k}$ symmetry). We denote the sets of admissible gate weights on each group by \mathcal{W}_O and \mathcal{W}_S , and the set of admissible total weights by $\mathcal{W}_{\text{total}} (\equiv \mathcal{W})$. The three weight-separation parameters ($s_{\text{total}}, s_O, s_S$) for these sets,

$$\mathcal{W}_i = \{w : w \equiv 1 \pmod{s_i}\} \quad i \in \{O, S, \text{total}\}, \quad (5)$$

can be chosen independently. A gate is labeled by the pair (w_O, w_S) with $w_O \in \mathcal{W}_O$, $w_S \in \mathcal{W}_S$, $w_O + w_S \in \mathcal{W}_{\text{total}}$. Each gate type $(w_O, w_S) \in \mathcal{W}$ carries a sign $\sigma_{w_O, w_S} \in \{+1, -1\}$: gates of type (w_O, w_S) implement $Z^{\otimes(w_O + w_S)}(\sigma_{w_O, w_S} \theta)$, i.e., the rotation angle is $+\theta$ when $\sigma_{w_O, w_S} = +1$ and $-\theta$ when $\sigma_{w_O, w_S} = -1$. The sign assignment is part of the circuit specification.

By the $S_k \times S_{n-k}$ symmetry, the phase accumulated by a basis state depends only on the Dicke-sector indices (i_O, i_S) : the Hamming weights on the output and check blocks. We denote this phase $\Phi(i_O, i_S)$.

Lemma 4 (Asymmetric Dicke-sector phase). *Assuming the borrowed-identity condition is satisfied at all (i'_O, i'_S) with $i'_O + i'_S < i_O + i_S$, the phase at Dicke sector (i_O, i_S) is*

$$\begin{aligned} \Phi(i_O, i_S) \equiv & (-1)^{i_O + i_S + 1} 2^{i_O + i_S} \theta \sum_{(w_O, w_S) \in \mathcal{W}} \sigma_{w_O, w_S} \\ & \times \binom{k - i_O}{w_O - i_O} \binom{n - k - i_S}{w_S - i_S} \pmod{2\pi}. \end{aligned} \quad (6)$$

Proof by induction on $i_O + i_S$ via Pascal's recurrence on both blocks; see App. C.

Theorem 5 (Asymmetric master condition). *A two-group circuit with gate types \mathcal{W} and signs $\{\sigma_{w_O, w_S}\} \subset \{+1, -1\}$ is a borrowed identity if and only if*

$$\sum_{(w_O, w_S) \in \mathcal{W}} \sigma_{w_O, w_S} \binom{k - i_O}{w_O - i_O} \binom{n - k - i_S}{w_S - i_S} \in 2^{l - i_O - i_S + 1} \mathbb{Z} \quad (7)$$

for all (i_O, i_S) with $i_O + i_S \leq l$. The condition is vacuous for other values of $i_O + i_S > l$ as for these values, Eq. (6) is automatically an integer multiple of 2π .

Equation (7) is linear in $\{\sigma_{w_O, w_S}\}$ over $\mathbb{Z}_{2^{l+1}}$, allowing the validity of any sign assignment to be verified in $O(k(n - k))$ time per Dicke sector. The output magic state is extracted by removing all gates of type $(w_O, 0)$ with $w_O \in \mathcal{W}_O \cap \mathcal{W}_{\text{total}}$. If the borrowed identity comprises N_{circuit} gates, the resulting input magic-state count is

$$N = N_{\text{circuit}} - \sum_{w \in \mathcal{W}_O \cap \mathcal{W}_{\text{total}}} \binom{k}{w}. \quad (8)$$

We present our search results, based on Eqs. [6–8], in Fig. 1, where the outputs are classified into Clifford equivalence classes [15] (see App. D): factories whose outputs differ by a Clifford circuit are grouped together [35]. Details, including the deterministic sign assignment (no search over signs is needed), are in App. F. We fix $s_S = 1$. Since every gate surviving the $(w_O, 0)$ removal touches a check qubit, single errors are always caught, guaranteeing distance 2; choosing $s_O = s_S$ reproduces the distance-2 and 3 symmetric families. Reaching arbitrary distance d at $k > 1$ requires breaking the check-qubit symmetry so that the smallest set of gates with cancelling check-supports has size d ; we leave this to future work.

The full sweep—runtime, scaling, and per-level catalogue—is detailed in App. F, with the $[[20, 4, 2]]$ factory worked out in App. E. By contrast, the Nezami–Haah classification [26] enumerates affine equivalence classes of Reed–Muller polynomials, a space growing exponentially in N ($\sim 5 \times 10^{12}$ candidates at $N \leq 38$) and specialized to $l = 3$. Within one search space we recover, at $k > 1$, both unentangled T -output factories and entangled CS/CCZ factories, families that earlier searches could reach only one at a time. Fig. 1 shows the density of factories over (N, k) for $N \leq 100$; Tables I–III list $N \leq 30$ representatives, and App. F details how the families of Fig. 1 (Bravyi–Haah, H-code/Iceberg, generalized triorthogonal, and distance-2 Nezami–Haah, including codes with $N \geq 1000$) are recovered. Notably, the search finds the $[[24, 6, 2]]$ and $[[12, 2, 2]]$ factories: a 6-qubit state Clifford-equivalent to two CCZ states, and a 2-qubit state Clifford-equivalent to one CS state, respectively. These match the $\text{CCZ}(8) \rightarrow \text{CCZ}(2)$ and $\text{CS}(4) \rightarrow \text{CS}(1)$ factories derived from algebraic-geometry (AG) codes [24].

We now turn to factories unreachable by the two-group symmetric search at $l = 3$, to show how its symmetry restricts the hunt for all distance-2 circuits. The Campbell–Howard synthillation families [15]—the T-to-CCZ family $[[6m + 2, 3m, 2]]$ ($[[14, 6, 2]]$, QUIRK) and the T-to-CS family $[[6m + 6, 2m, 2]]$ ($[[18, 4, 2]]$, QUIRK)—both break the two-group symmetry: their gate sets are not symmetric over the outputs. The T-to-CCZ family is realized with pure $\pi/8$ rotations; the T-to-CS family additionally uses multi-weight phase rotations of type $(i \leq l)$ $c\pi/2^i$ rotations ($c \in \mathbb{Z}_{2^i}$)—the extended borrowed-identity formalism which is not restricted to $i = l$ —to reach its

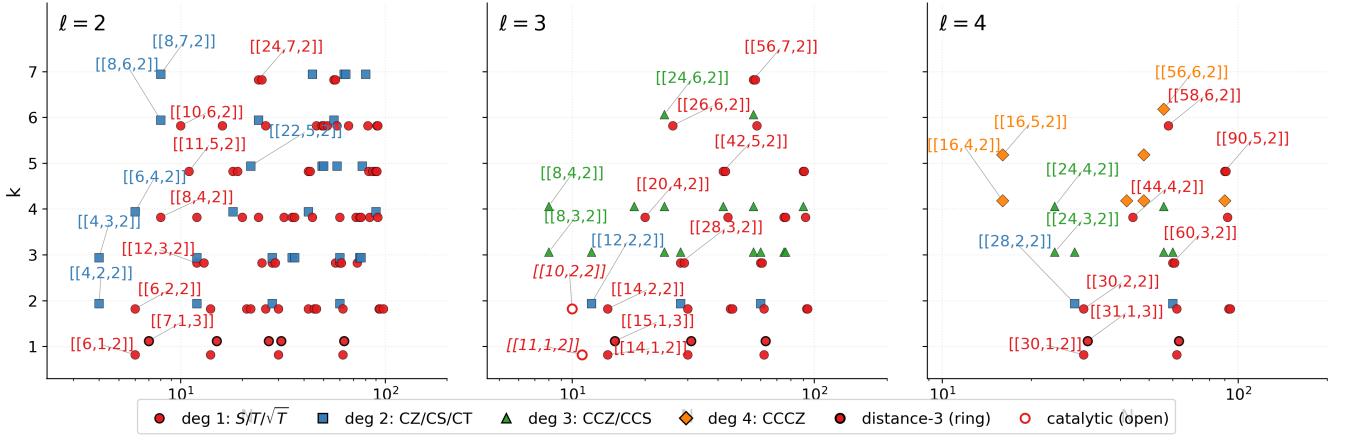


FIG. 1. **Distillation factories recovered by the two-group search.** Each marker is a factory at (N, k) : N magic states of type $Z^{\otimes w}(\pi/2^l)$ yielding a k -qubit output, at Clifford-hierarchy levels $l \in \{2, 3, 4\}$ (three panels). Marker shape and color encode the output type as listed in the legend (see App. D for output classification). All markers are distance-2 except the bold-ringed $k = 1$ markers, which are distance-3. Filled markers are produced by the two-group search over the swept range $k \leq 7$, $n \leq 11$, $s_{\text{total}}, s_O \leq 7$ (App. F); open markers are the non-CSS factories, which the search does not produce but fall under the borrowed identity framework. In each column the top panel shows $N \leq 100$ with the canonical (smallest- N) representative annotated per degree and k ; the full extent ($N > 1000$) is shown in Fig. 2, with parameter tuples for $N \leq 30$ factories listed in Tables I–III for explicit circuit construction.

optimal T -count. The two Quirk circuits linked above make clear that these factories require breaking the two-group symmetry constraint. As an existence proof, we built a symmetry-free, targeted-output search that solves the borrowed-identity condition directly for a chosen output at levels $l \in \{2, 3, 4\}$ (App. H). In addition to the above families, it also finds factories with mixed outputs, like $[[18, 5, 2]]$ (QUIRK) which yields one CS and one CCZ, not found explicitly in the synthillation literature, so the borrowed-identity picture handles mixed-output factories too.

The ultimate goal for this formalism is a *tractable* search that captures the smallest factory at each distance for different types of magic states. This is motivated by the growing use of the $[[8, 3, 2]]$ factory—which has the smallest number of input qubits—in recent resource estimates of fault-tolerant quantum computing [6, 7]. The payoff of searching across types is that factory size depends strongly on both the output and the input: distilling input T states into CCZ and CS outputs can admit smaller factories than T (with non-CSS constructions smaller still), while distilling from higher-level inputs such as CS-to-CS or CCZ-to-CCZ costs more than the corresponding T -input factory. At distance-2, the smallest factory of each output type is already covered by our two-group symmetric search; the batched synthillation factories above, while also distance-2, are larger multi-output variants that the symmetry-free targeted-output search can reach. For higher-distance we would need to break the symmetry, as discussed below Eq. (8).

c. Malleable circuits— Restricting the previous construction to $|\mathcal{S}| = 1$, we can analytically derive that

$k = n - 1$ yields $[[2^n - 2^{n-1}, n - 1, 2]] = [[2^{n-1}, n - 1, 2]]$ factories for $s_O = s_S = s_{\text{total}} = 1$. This is equivalent to constructing a partial borrowed identity on the output qubits \mathcal{O} —with each gate additionally conditioned on the single check qubit in \mathcal{S} —leaving the check qubit unentangled at the end. In this section we discuss the effects of applying this procedure sequentially: at each step j , the unentangled check qubit from the previous step is eliminated, and a new qubit from \mathcal{O}_{j-1} is promoted to the single check qubit in \mathcal{S}_j . After $j = n$ steps, the complete parent circuit reduces to the symmetric borrowed identity at level l with $s = s_{\text{total}} = 1, 2$, i.e., a solution of Theorem 3. Specifically, after sequence step j , the resulting factory is $[[2^{n-s+1} - 2^{n-j-s+1}, n - j, 2]]$, with the $k = 1$ endpoint ($j = n - 1$) at distance 3 for $s = 2$.

For $n_{\text{min}} = l + 1$, the minimum n for an $s = 1$ symmetric solution, the sequential construction reveals the output magic-state type directly. After step j , the factory $[[2^{l+1} - 2^{l+1-j}, l + 1 - j, 2]]$ has an output state whose unitary preparation requires the same number of T gates as the number of gates removed from the n_{min} symmetric borrowed identity at $s = 1$, namely $2^{l+1-j} - 1$. These factories are already recovered by the asymmetric search; we highlight them to illustrate *malleability* (for example, at $l = 2$ the chain $[[4, 2, 2]] \rightarrow [[6, 1, 2]]$ gives outputs $|CZ\rangle$ then $|S\rangle$).

Proposition 6 (Factory malleability). *A single borrowed identity circuit on n qubits encodes multiple distinct distillation factories. The output magic-state type is determined by which gates are removed, not by the circuit itself.*

We illustrate this with two concrete families for $l = 3$, for which we have provided annotated circuits in App. I, in addition to the active Quirk [36] links throughout the main text.

Four-qubit malleable family. For $l = 3$, the closed-form solution for symmetric circuits at $s = 1$ yields $n_{\min} = 4$, and thus the output at step j requires $2^{4-j} - 1$ T states for unitary preparation. The single four-qubit borrowed identity (QUIRK) yields five distinct factories spanning all three magic states T , CS and CCZ :

- Remove all weight- ≤ 3 gates on the output block: $[[8, 3, 2]]$ with output $|CCZ\rangle \equiv 7$ T states (QUIRK).
- Sequential step $j = 2$ on the same parent: $[[12, 2, 2]]$ with output $|CS\rangle \equiv 3$ T states (QUIRK).
- Sequential step $j = 3$: $[[14, 1, 2]]$ with output $|T\rangle$ (QUIRK).
- Apply $|CCZ\rangle \rightarrow |T\rangle$ catalytic conversion after step $j = 1$, retaining the check qubit (performing check on the output qubits): $[[11, 1, 2]]$ yields output $|T\rangle$ (QUIRK).
- Same catalytic conversion but now retaining two output qubits, and measure one output qubit to disentangle the magic states: $[[10, 2, 2]]$ with two $|T\rangle$ outputs (QUIRK).

Of these, $[[8, 3, 2]]$ [11, 12, 37] and $[[10, 2, 2]]$ [16] are known; $[[11, 1, 2]]$ is introduced here. The framework recovers all five as endpoints of one parent. The two catalytic factories use Clifford gates in addition to the components of a borrowed identity circuit—hence non-CSS—and lower the input T -count: the catalytic conversion uses entangling gates already contained in the extended borrowed identity, while the Hadamard gates are a new addition.

Five-qubit malleable family. Note that symmetric circuits with $k > 1$ cannot have distance $d > 2$ even for the $s = 2$ case, yielding $[[2^{l+1} - 2^{l+1-j}, l + 2 - j, 2]]$ factories (since $n_{\min} = l + 2$ for $s = 2$). The five-qubit parent identity (QUIRK) extends construction to higher k and to distance-3 endpoints:

- $j = 1$: $[[8, 4, 2]]$ with CCZ -equivalent output (QUIRK).
- $j = 2$: $[[12, 3, 2]]$ with CCZ -equivalent output (QUIRK).
- $j = 3$: $[[14, 2, 2]]$ with two output $|T\rangle$ (QUIRK).
- $j = 4$: $[[15, 1, 3]]$ with a single output $|T\rangle$ but at increased distance, as distance-3 is retained for $k = 1$ (QUIRK).

This five-qubit circuit shows that adding qubits need not raise the output T -count: $[[8, 4, 2]]$ ($s=3, n=5, k=4$) has the same catalytic T -count as $[[8, 3, 2]]$ and an output in

the same Clifford equivalence class, but its extra qubits give redundant detection of correlated errors that escape the four-qubit realization (App. I)—quantifying when this is worth the qubit cost is left open.

At $l = 4$ the $n = 5$ parent gives $[[16, 4, 2]] \rightarrow [[24, 3, 2]] \rightarrow [[28, 2, 2]] \rightarrow [[30, 1, 2]]$ ($CCCZ$, CCS , CT , \sqrt{T}) and the $[[31, 1, 3]]$ endpoint at $s = 2$. The sequential search yields no factories beyond the asymmetric one; it is formalized, with worked four- and five-qubit parent circuit examples, in App. G. However, the malleability introduced by the sequential construction has a direct consequence for fault-tolerant compilation: the choice of output magic state within a Clifford hierarchy level l need not be fixed at hardware design time. A compiler can defer this decision to compilation time, specializing the same parent template to whichever resource state the surrounding computation requires; Heisenberg-picture constructions, which fix the output gate in the code itself, offer no such knob.

Discussion— We have presented a unified Schrödinger-picture framework for magic-state distillation. A single borrowed-identity condition, holding at every Clifford level through $\theta = \pi/2^l$, reaches three classes of factory within one search space (Fig. 1): unentangled T -output factories from the symmetric and two-group searches, entangled-output factories from the sequential construction (e.g. the $[[2^l, l, 2]]$ family [21, 22]), and non-CSS catalytic factories from Clifford+ T conversion. The symmetric case is closed-form, recovering the Reed–Muller chain $[[2^{l+1} - 1, 1, 3]]$ at distance 3 for every l . Its structural payoff is *malleability*: one parent circuit on n qubits encodes many factories, so the output magic-state type is chosen at compile time by gate removal rather than fixed at hardware design—with no analogue in Heisenberg-picture frameworks (Figs. 5–6).

Three open questions remain towards the goal of most general yet tractable search of distillation factories. The first and foremost goal is to find the smallest *multi-output* ($k > 1$) magic state factories, for each Clifford level, at distances $d > 2$ —the true analogues of $[[8, 3, 2]]$ at higher distance. Higher distance at $k = 1$ is already accessible to general-purpose solvers [38]; the open problem is the smallest multi-output factory at $d > 2$, which requires breaking the check-qubit symmetry so that the smallest set of gates with cancelling check-supports has size d while retaining more than one output, a gate-weight assignment beyond Theorem 5, as noted below Eq. (8). Whether this can be done by an exhaustive search based on extended borrowed identities without sacrificing its linear, level-uniform structure is open. Adding *Hadamard gates* to the extended borrowed identity formalism, a single non-diagonal primitive, is equally important since it reaches non-CSS factories such as $[[10, 2, 2]]$ [16] and the synthillation circuits through a systematic search, at higher rate and distance, not possible in any search

known yet. Finally, the close correspondence between purely non-Clifford borrowed identities and code-based constructions hints at an *automorphism* between them, a map that would place many known factories within our framework. Together these directions point toward a single algebraic foundation for distillation across all Clifford levels and output types, and a sharper boundary between the Schrödinger- and Heisenberg-picture approaches.

Code and Data Availability— All circuits are available via the Quirk [36] links in the text and appendices; the search code and complete output ($N \geq 1000$) are at Ref. [39].

Note Added— While preparing this manuscript, we became aware of concurrent and independent work [38] studying compact distillation factories via a repetition-code, SAT-based search, establishing no-go theorems and single-output ($k = 1$) protocols at distance ≥ 3 . Single-output factories at higher distance are likewise within reach of the borrowed identity framework through a slow SAT search; our focus for this work was instead a fast exhaustive search on the multi-output ($k > 1$) regime and the malleability between factories distilling different magic states at the same Clifford level.

Acknowledgements— SS would like to thank the Google student research 2024 program. SS also acknowledges discussions with Anqi Gong and Shubham Jain.

* Present address: IBM Quantum, IBM T. J. Watson Research Center, Yorktown Heights, NY 10598, USA; Corresponding address: shraggygkp@gmail.com

- [1] S. Bravyi and A. Kitaev, *Phys. Rev. A* **71**, 022316 (2005), introduces magic-state distillation and the $[[15, 1, 3]]$ Reed-Muller protocol; also the $[[5, 1, 3]]$ $|T\rangle$ -distillation routine.
- [2] B. Eastin and E. Knill, *Physical review letters* **102**, 110502 (2009).
- [3] D. Gottesman and I. L. Chuang, *Nature* **402**, 390 (1999).
- [4] P. Sales Rodriguez, J. M. Robinson, P. N. Jepsen, Z. He, C. Duckering, C. Zhao, K.-H. Wu, J. Campo, K. Bagnall, M. Kwon, *et al.*, *Nature* **645**, 620 (2025).
- [5] A. G. Fowler, M. Mariantoni, J. M. Martinis, and A. N. Cleland, *Phys. Rev. A* **86**, 032324 (2012).
- [6] C. Gidney and M. Ekerå, *Quantum* **5**, 433 (2021), 1905.09749.
- [7] H. Zhou, C. Duckering, C. Zhao, D. Bluvstein, M. Cain, A. Kubica, S.-T. Wang, and M. D. Lukin, in *Proceedings of the 52nd Annual International Symposium on Computer Architecture* (2025) pp. 1432–1448.
- [8] S. Bravyi and J. Haah, *Phys. Rev. A* **86**, 052329 (2012), triorthogonal codes; introduces the $[[3k + 8, k, 2]]$ family. The $k = 2$ instance is $[[14, 2, 2]]$ and the $k = 4$ instance is $[[20, 4, 2]]$, 1209.2426.
- [9] N. Rengaswamy, R. Calderbank, M. Newman, and H. D. Pfister, *IEEE J. Sel. Areas Inf. Theory* **1**, 499 (2020), 1910.09333.
- [10] J. Haah and M. B. Hastings, *Quantum* **2**, 71 (2018), generalised triorthogonal codes for T , CS, CCZ distillation., 1709.02832.
- [11] H. Bombin and M. A. Martin-Delgado, *Phys. Rev. B* **75**, 075103 (2007), introduces the 3D color code; the smallest instance is the $[[8, 3, 2]]$ code on the cube, with transversal T implementing logical CCZ., cond-mat/0607736.
- [12] B. Eastin, *Phys. Rev. A* **87**, 032321 (2013), first $8T \rightarrow$ CCZ (Toffoli) distillation factory using the $[[8, 3, 2]]$ code of Ref. [11], 1212.4872.
- [13] A. Krishna and J.-P. Tillich, *Phys. Rev. Lett.* **123**, 070507 (2019), 1811.08461.
- [14] A. Wills, M.-H. Hsieh, and H. Yamasaki, arXiv preprint (2024), 2408.07764.
- [15] E. T. Campbell and M. Howard, *Phys. Rev. A* **95**, 022316 (2017), 1606.01904.
- [16] A. M. Meier, B. Eastin, and E. Knill, *Quantum Inf. Comput.* **13**, 195 (2013), the original $[[10, 2, 2]]$ ($10 \rightarrow 2$) protocol using the $[[4, 2, 2]]$ code as inner block., 1204.4221.
- [17] C. Jones, *Phys. Rev. A* **87**, 042305 (2013), introduces the $[[n, n - 4, 2]]$ “H-code” family of which $[[6, 2, 2]]$ is the smallest member., 1210.3388.
- [18] D. Litinski, *Quantum* **3**, 205 (2019), space-time-optimised distillation circuits including explicit $15 \rightarrow 1$, $20 \rightarrow 4$, $14 \rightarrow 2$, and $8 \rightarrow$ CCZ realisations on the surface code; the $[[14, 2, 2]]$ entry in our table is the small-footprint variant introduced here., 1905.06903.
- [19] D. Gottesman, *Phys. Rev. A* **54**, 1862 (1996).
- [20] C. Jones, *Phys. Rev. A* **87**, 022328 (2013), 1212.5069.
- [21] A. Barg, N. J. Coble, D. Hangleiter, and C. Kang, *IEEE Transactions on Information Theory* **72**, 415 (2026).
- [22] M. A. Webster, B. J. Brown, and S. D. Bartlett, *Quantum* **6**, 815 (2022).
- [23] M. A. Webster, A. O. Quintavalle, and S. D. Bartlett, *New Journal of Physics* **25**, 103018 (2023).
- [24] A. Gong, Magic state distillation via codes over binary extension fields, Oral presentation at the Quantum Error Correction 2026 conference (2026).
- [25] This is the number of valid borrowed-identity solutions found, i.e. admissible (parameter-tuple, sign) configurations; it includes solutions with trivial (stabilizer) output and counts the same factory once for each (n, s) tuple realizing it, so it exceeds the number of distinct factories.
- [26] S. Nezami and J. Haah, *Phys. Rev. A* **106**, 012437 (2022), 2107.09684.
- [27] S. X. Cui, D. Gottesman, and A. Krishna, *Phys. Rev. A* **95**, 012329 (2017), 1608.06596.
- [28] S_n acts by relabeling qubit registers, not by physically permuting hardware: qubits with identical circuit connectivity are interchangeable for the borrowed-identity condition.
- [29] Even weights cannot yield $k = 1$ factories.
- [30] A. M. Steane, *Phys. Rev. A* **54**, 4741 (1996).
- [31] A. Steane, *Proceedings of the Royal Society of London. Series A: Mathematical, Physical and Engineering Sciences* **452**, 2551 (1996).
- [32] A. Gong and J. M. Renes, arXiv preprint arXiv:2410.23263 (2024).
- [33] L. Luo, Z. Ma, D. Lin, and H. Wang, *Quantum Science & Technology* **5**, 045022 (2020).
- [34] A. Kubica and M. E. Beverland, *Physical Review A* **91**, 032330 (2015).
- [35] E.g. $[[8, 4, 2]]$ at $l = 3$ is a Clifford-padded version of the cube $[[8, 3, 2]]$; it is retained as a distinct CCZ-class factory, since the extra qubit yields additional correlated-error detection (Fig. 6(b)).

- [36] C. Gidney, *Quirk: A drag-and-drop quantum circuit simulator*. (2016).
- [37] C. Jones, *Phys. Rev. A* **87**, 052334 (2013), independent and concurrent $8T \rightarrow \text{CCZ}$ construction using the $[[8, 3, 2]]$ code of Ref. [11]; refined two-round error detection., 1303.6971.
- [38] H. Jacinto, X. Valcarce, V. Barizien, É. Gouzien, and N. Sangouard, arXiv preprint arXiv:2606.07734 (2026).
- [39] S. Singh, *Algebraic magic state factory search* [GitHub] (2026).

Appendix A: Schrödinger vs. Heisenberg picture: specialization to triorthogonality

Proposition 7. *Every transversal- T distillation circuit on a CSS code is, under spacetime duality, a borrowed identity. The converse fails: the catalytic factories $[[10, 2, 2]]$ and $[[11, 1, 2]]$ constructed in Sec. 0c are borrowed identities whose construction includes Clifford+ T post-processing and therefore does not arise as the transversal T of any CSS code.*

The strict containment is the source of the framework's reach. The specialization of the borrowed-identity condition to triorthogonality (transversal T at $l = 3$) and quasitransversality [15] via the duality is detailed in this Appendix.

a. Heisenberg picture. For a CSS code with X -stabilizer group generated by $\{X^{\otimes b_1}, \dots, X^{\otimes b_n}\}$ on N physical qubits, the action of $T^{\otimes N}$ on each generator follows from $TXT^\dagger = (X + Y)/\sqrt{2}$:

$$TX^{\otimes b}T^\dagger = X^{\otimes b} \cdot O_b, \quad (\text{A1})$$

with O_b a Z -polynomial on the support of b . For $T^{\otimes N}$ to implement a logical T gate, each O_b must act as

$$O_b = \frac{I + i\sqrt{2}Z_L}{2^{|b|/2}}, \quad (\text{A2})$$

pinning O_b on both $|\pm\rangle_L$. This is the triorthogonality condition of Ref. [8]; the matrix search of Ref. [26] enumerates solutions.

b. Spacetime dual. Under spacetime rotation, the N physical qubits become N multi-qubit Z -rotations, the n X -stabilizer checks become n qubits prepared in $|+\rangle$, and the transversal $T^{\otimes N}$ becomes the application of N rotations $Z^{\otimes b_i}(\pi/4)$ in time. The $+1$ outcome of all X -stabilizer measurements in the original picture correspond, in the dual, to the borrowed-identity condition $\mathcal{C}|+\rangle^{\otimes n} = e^{i\phi}|+\rangle^{\otimes n}$.

Appendix B: Proof of Lemma 2 (Dicke-sector phase accumulation) and distance guarantees

We prove Eq. (3) by induction on i . Direct counting of how many gates flip a given basis element of the Dicke

sector $| \binom{n}{i} \rangle$ gives the starting form

$$\Phi(i) = 2\theta \sum_{\substack{m \in 2\mathbb{Z}+1 \\ m \leq i}} \binom{i}{m} \sum_{\substack{w \in \mathcal{W} \\ w \geq m}} \binom{n-i}{w-m}, \quad (\text{B1})$$

where m counts the number of designated qubits in the support of a weight- w gate that overlap with the i flipped qubits; the parity of m determines whether the gate contributes 2θ or 0 phase.

a. Base case $i = 1$. The only odd $m \leq 1$ is $m = 1$, so

$$\Phi(1) = 2\theta \sum_{w \in \mathcal{W}} \binom{n-1}{w-1} = 2^1\theta \sum_{w \in \mathcal{W}} \binom{n-1}{w-1}, \quad (\text{B2})$$

matching Eq. (3) at $i = 1$.

b. Inductive step. Assume $\Phi(j) \equiv 0 \pmod{2\pi}$ for all $j < i$. Apply Pascal's recurrence $\binom{n-i}{w-m} = \binom{n-i+1}{w-m} - \binom{n-i}{w-m-1}$ exactly $i-m$ times, raising the bottom binomial index from $w-m$ to $w-i$:

$$\binom{n-i}{w-m} = \sum_{r=0}^{i-m} (-1)^r \binom{i-m}{r} \binom{n-m-r}{w-m-r}. \quad (\text{B3})$$

Substituting into Eq. (B1), setting $j = m + r$, and re-ordering the double sum gives

$$\begin{aligned} \Phi(i) &= 2\theta \sum_{\substack{j = \text{Im odd} \\ m \leq j}}^i \sum_{\substack{m \leq j}} (-1)^{j-m} \binom{i}{m} \binom{i-m}{j-m} \\ &\quad \times \sum_{\substack{w \in \mathcal{W} \\ w \geq j}} \binom{n-j}{w-j}. \end{aligned} \quad (\text{B4})$$

The identity $\binom{i}{m} \binom{i-m}{j-m} = \binom{i}{j} \binom{j}{m}$ collects the inner-sum coefficient at each j as

$$C(i, j) = 2\theta \binom{i}{j} \sum_{\substack{m \text{ odd} \\ m \leq j}} (-1)^{j-m} \binom{j}{m}. \quad (\text{B5})$$

At $j = i$, the standard odd-extraction identity $\sum_{m \text{ odd}} \binom{j}{m} = 2^{j-1}$ gives $C(i, i) = 2^i\theta$. For $j < i$, $C(i, j)$ is proportional to $\Phi(j)$ with integer coefficient $\binom{i}{j}$; by the inductive hypothesis these terms vanish modulo 2π . Only the $j = i$ term survives, yielding Eq. (3). \square

c. Distance saturation. For $s \geq 3$ the distance saturates at $d = 3$: two equal-weight gates always overlap oddly on two qubits, and adjoining a weight-1 gate on one of them leaves a single-qubit odd overlap—if the output lives there, a combination of three gate errors goes undetected.

Appendix C: Proof of Lemma 4 (Asymmetric Dicke-sector phase)

We prove Eq. (6) by induction on $i_O + i_S$, extending Lemma 2 from one Dicke index to two. The argument

follows the same three-step structure as App. B — Pascal’s recurrence to raise binomial indices, the identity $\binom{i}{m} \binom{i-m}{j-m} = \binom{i}{j} \binom{j}{m}$ to refactor the double sum, and an odd-extraction identity to evaluate the parity-restricted inner sum — now applied block-by-block, with the two blocks connected only by the parity constraint on the total overlap $m_O + m_S$.

Per the definition of weight- w rotation gate in Eq. (2), a weight- (w_O, w_S) gate with sign σ_{w_O, w_S} contributes phase $2\sigma_{w_O, w_S} \theta$ to a basis element of Dicke sector (i_O, i_S) when its overlap m_O with the i_O flipped output qubits and overlap m_S with the i_S flipped check qubits satisfies $m_O + m_S$ odd, and phase 0 otherwise. The number of weight- (w_O, w_S) gates with overlap (m_O, m_S) is $\binom{i_O}{m_O} \binom{k-i_O}{w_O-m_O} \binom{i_S}{m_S} \binom{n-k-i_S}{w_S-m_S}$. Summing over all gate types and all odd-parity overlaps gives the starting form

$$\begin{aligned} \Phi(i_O, i_S) &= 2\theta \sum_{(w_O, w_S) \in \mathcal{W}} \sigma_{w_O, w_S} \sum_{\substack{m_O+m_S \text{ odd} \\ m_O \leq i_O, m_S \leq i_S}} \binom{i_O}{m_O} \binom{i_S}{m_S} \\ &\quad \times \binom{k-i_O}{w_O-m_O} \binom{n-k-i_S}{w_S-m_S}. \end{aligned} \quad (\text{C1})$$

a. Base cases. The $(i_O, i_S) = (0, 0)$ case is trivial, so we verify Eq. (6) at the two smallest sectors of $i_O + i_S = 1$: $(i_O, i_S) = (1, 0)$ and $(0, 1)$.

At $(1, 0)$: the constraint “ $m_O + m_S$ odd with $m_O \leq 1, m_S \leq 0$ ” forces $m_O = 1, m_S = 0$, so Eq. (C1) becomes

$$\Phi(1, 0) = 2\theta \sum_{(w_O, w_S) \in \mathcal{W}} \sigma_{w_O, w_S} \binom{1}{1} \binom{0}{0} \binom{k-1}{w_O-1} \binom{n-k}{w_S}, \quad (\text{C2})$$

which simplifies to $2\theta \sum \sigma_{w_O, w_S} \binom{k-1}{w_O-1} \binom{n-k}{w_S}$ — matching the prefactor $(-1)^{1+0+1} 2^{1+0} \theta = 2\theta$ of Eq. (6) at $(1, 0)$ with binomial factors $\binom{k-1}{w_O-1} \binom{n-k}{w_S}$. By symmetry, the analogous identity holds at $(0, 1)$.

b. Inductive step. Assume Eq. (6) holds, and equals zero modulo 2π by the borrowed-identity hypothesis, for all (i'_O, i'_S) with $i'_O + i'_S < i_O + i_S$. We show Eq. (6) also holds at (i_O, i_S) .

The strategy parallels App. B: use Pascal’s recurrence on both blocks to reorganize Eq. (C1) into a sum of contributions indexed by sectors $(j_O, j_S) \leq (i_O, i_S)$. Iterating the recurrence $\binom{k-i_O}{w_O-m_O} = \binom{k-i_O+1}{w_O-m_O} - \binom{k-i_O}{w_O-m_O-1}$ exactly $i_O - m_O$ times on the output block, and analogously $i_S - m_S$ times on the check block, gives

$$\binom{k-i_O}{w_O-m_O} = \sum_{j_O=m_O}^{i_O} (-1)^{j_O-m_O} \binom{i_O-m_O}{j_O-m_O} \binom{k-j_O}{w_O-j_O}, \quad (\text{C3})$$

$$\binom{n-k-i_S}{w_S-m_S} = \sum_{j_S=m_S}^{i_S} (-1)^{j_S-m_S} \binom{i_S-m_S}{j_S-m_S} \binom{n-k-j_S}{w_S-j_S}. \quad (\text{C4})$$

Substituting into Eq. (C1) and applying the binomial identity $\binom{i_O}{m_O} \binom{i_O-m_O}{j_O-m_O} = \binom{i_O}{j_O} \binom{j_O}{m_O}$ (and analogously

for the check block), the contribution at fixed (j_O, j_S) factorizes as a product of three pieces: a sign and prefactor $(-1)^{j_O+j_S+1} 2\theta \binom{i_O}{j_O} \binom{i_S}{j_S}$ [the overall -1 from $(-1)^{m_O+m_S} = -1$ on every odd-parity term, which can be pulled out of the (m_O, m_S) sum], a combinatorial weight

$$\sum_{\substack{m_O+m_S \text{ odd} \\ m_O \leq j_O, m_S \leq j_S}} \binom{j_O}{m_O} \binom{j_S}{m_S} = \begin{cases} 2^{j_O+j_S-1} & j_O + j_S \geq 1, \\ 0 & j_O + j_S = 0, \end{cases} \quad (\text{C5})$$

[obtained by splitting odd parity into “ m_O even, m_S odd” and “ m_O odd, m_S even” and applying $\sum_{m \text{ even}} \binom{j}{m} = \sum_{m \text{ odd}} \binom{j}{m} = 2^{j-1}$ for $j \geq 1$], and a gate-type sum $\sum_{(w_O, w_S) \in \mathcal{W}} \sigma_{w_O, w_S} \binom{k-j_O}{w_O-j_O} \binom{n-k-j_S}{w_S-j_S}$.

The full expression at (j_O, j_S) therefore reduces to $\binom{i_O}{j_O} \binom{i_S}{j_S}$ times the closed-form right-hand side of Eq. (6) evaluated at (j_O, j_S) — i.e., to $\binom{i_O}{j_O} \binom{i_S}{j_S} \cdot \Phi(j_O, j_S)$. For $(j_O, j_S) \neq (i_O, i_S)$ with $j_O + j_S \geq 1$, this is an integer multiple of $\Phi(j_O, j_S)$, which vanishes modulo 2π by the inductive hypothesis. The $(0, 0)$ contribution vanishes from Eq. (C5). Only the top-sector contribution at $(j_O, j_S) = (i_O, i_S)$ survives, yielding Eq. (6). \square

Appendix D: Output-state classification via residual phase

Setting $i_S = 0$ in Lemma 4, the residual phase $\Phi'(i_O, 0)$ depends only on the Hamming weight $i_O = |x|$ of the output qubits, so the output state is

$$|\Psi_{\text{out}}\rangle = \frac{1}{\sqrt{2^k}} \sum_{x \in \{0,1\}^k} e^{i\Phi'(|x|, 0)} |x\rangle, \quad (\text{D1})$$

with $\Phi'(0, 0) = 0$. Define the d -th iterated finite difference of $\Phi'(\cdot, 0)/\theta$ at 0 as

$$\Delta^d \left[\frac{\Phi'(\cdot, 0)}{\theta} \right] (0) := \sum_{j=0}^d (-1)^{d-j} \binom{d}{j} \frac{\Phi'(j, 0)}{\theta}. \quad (\text{D2})$$

Proposition 8. $|\Psi_{\text{out}}\rangle$ contains, as its dominant entangling content, a d -qubit level- l Clifford-hierarchy resource — non-Clifford (magic) precisely for $l \geq 3$ — where d is the largest index in $\{1, \dots, k\}$ for which (D2) is non-zero modulo 2^{l+1} .

Proof. The inductive step of Lemma 4 shows that $\Phi'(i_O, 0)/\theta$ receives a non-vanishing contribution only from the top sector $(j_O, j_S) = (i_O, 0)$, with all lower sectors cancelling by the borrowed-identity condition. The binomial factor $\binom{i_O}{j_O} \binom{i_S}{j_S} \Big|_{i_S=j_S=0} = \binom{i_O}{j_O}$ at $j_O = d$ is precisely the degree- d Newton basis element, so Eq. (6) at $i_S = 0$ is already the Newton expansion

$$\frac{\Phi'(i_O, 0)}{\theta} = \sum_{d=1}^k \Delta^d \left[\frac{\Phi'(\cdot, 0)}{\theta} \right] (0) \binom{i_O}{d}. \quad (\text{D3})$$

Each degree- d term corresponds to a symmetric layer of d -qubit diagonal gates applied to all size- d subsets of the output qubits. Following Ref. [15], such a layer realizes a level- l diagonal gate—non-Clifford (magic) precisely for $l \geq 3$ —if and only if its Newton coefficient is non-zero modulo 2^{l+1} . The largest such d identifies the dominant resource; and is used to define the Clifford-equivalence classes, based on which the outputs are classified. \square

Appendix E: Example verifications

We verify the borrowed-identity and output-extraction conditions for two canonical factories: the sequential $[[8, 3, 2]]$ and the asymmetric $[[20, 4, 2]]$.

1. The $[[8, 3, 2]]$ factory ($n = 4, k = 3, l = 3$)

The $[[8, 3, 2]]$ factory (**QUIRK**) arises from the sequential construction at $j = 1$ with $\mathcal{W}_1 = \{1, 2, 3, 4\}$, $n = 4$, $\theta = \pi/8$.

a. Borrowed-identity check. The Dicke-sector condition (Lemma 2) at $i = 1$ requires $\sum_{w \in \mathcal{W}} \binom{3}{w-1} \in 2^{l-i+1}\mathbb{Z} = 8\mathbb{Z}$:

$$\binom{3}{0} + \binom{3}{1} + \binom{3}{2} + \binom{3}{3} = 1 + 3 + 3 + 1 = 8 \equiv 0 \pmod{8}. \quad (\text{E1})$$

Higher Dicke sectors $i \in \{2, 3\}$ give modulus exponents $l - i + 1 \in \{2, 1\}$, with the sum $\sum_w \binom{3}{w-i} \in \{4, 2\}$ respectively, both satisfying the relevant divisibility. The borrowed-identity gate count is $\binom{4}{1} + \binom{4}{2} + \binom{4}{3} + \binom{4}{4} = 15$.

b. Output extraction. Removing all gates of weight $w \leq k = 3$ whose support lies entirely on the three designated output qubits leaves $N = 15 - (\binom{3}{1} + \binom{3}{2} + \binom{3}{3}) = 15 - 7 = 8$ gates of types $(w_O, w_S) \in \{(0, 1), (1, 1), (2, 1), (3, 1)\}$. The residual phase on the output Dicke sectors, normalized so that $\Phi'(0)/\theta = 0$, evaluates to

$$\Phi'(i_O)/\theta \equiv \begin{cases} 0 & i_O = 0, \\ -8 & i_O = 1, 2, 3, \end{cases} \pmod{16}. \quad (\text{E2})$$

The third finite difference in i_O is constant and nonzero, identifying the residual as a degree-3 polynomial—the signature of $|\text{CCZ}\rangle$ output up to Clifford correction. \checkmark

2. The $[[20, 4, 2]]$ factory ($n = 7, k = 4, l = 3$)

We verify the asymmetric borrowed-identity condition at $(l, n, k) = (3, 7, 4)$, $\theta = \pi/8$, $(s_{\text{total}}, s_O, s_S) = (2, 3, 1)$.

a. Gate set. $\mathcal{W}_{\text{total}} = \{1, 3, 5, 7\}$, $\mathcal{W}_O = \{0, 1, 4\}$, $\mathcal{W}_S = \{0, 1, 2, 3\}$. The allowed pairs are $\mathcal{W} =$

$\{(0, 1), (0, 3), (1, 0), (1, 2), (4, 1), (4, 3)\}$. The borrowed-identity gate count is

$$\begin{aligned} N_{\text{circuit}} &= \binom{4}{0} \binom{3}{1} + \binom{4}{0} \binom{3}{3} + \binom{4}{1} \binom{3}{0} \\ &\quad + \binom{4}{1} \binom{3}{2} + \binom{4}{4} \binom{3}{1} + \binom{4}{4} \binom{3}{3} \\ &= 3 + 1 + 4 + 12 + 3 + 1 = 24. \end{aligned} \quad (\text{E3})$$

b. Sign assignment. The two-cell deterministic check of asymmetric circuits fails at the all-positive assignment. The second cell, with $\sigma_{0,1} = \sigma_{0,3} = -1$ on the check-only gates and $\sigma = +1$ on every gate touching at least one output qubit, satisfies Eq. (7); we verify this explicitly below.

c. Phase verification. By Lemma 4, the closed-form phase at sector (i_O, i_S) is

$$\begin{aligned} \Phi(i_O, i_S)/\theta &\equiv (-1)^{i_O+i_S+1} 2^{i_O+i_S} \\ &\quad \times \sum_{(w_O, w_S) \in \mathcal{W}} \sigma_{w_O, w_S} T_{w_O, w_S}^{(i_O, i_S)} \pmod{16}, \end{aligned} \quad (\text{E4})$$

where $T_{w_O, w_S}^{(i_O, i_S)} := \binom{k-i_O}{w_O-i_O} \binom{n-k-i_S}{w_S-i_S}$ is the gate-overlap binomial product, with $k = 4$, $n - k = 3$. For each of the six allowed pairs (w_O, w_S) , we tabulate $T_{w_O, w_S}^{(i_O, i_S)}$ at the relevant non-trivial Dicke sectors:

(i_O, i_S)	(0, 1)	(0, 3)	(1, 0)	(1, 2)	(4, 1)	(4, 3)
(0, 1)	1	1	0	8	1	1
(1, 0)	0	0	1	3	3	1
(0, 2)	0	1	0	4	0	1
(1, 1)	0	0	0	2	1	1
(1, 2)	0	0	0	1	0	1
(2, 1)	0	0	0	0	1	1
\vdots	(remaining sectors analogously)					

Multiplying each $T_{w_O, w_S}^{(i_O, i_S)}$ by the corresponding sign σ_{w_O, w_S} and the prefactor $(-1)^{i_O+i_S+1} 2^{i_O+i_S}$, the result at every (i_O, i_S) vanishes modulo 16. \checkmark

d. Output extraction. Removing the four $(1, 0)$ gates leaves $N = 20$ gates. The residual output phase satisfies

$$\Phi'(i_O, 0)/\theta = -2i_O \pmod{16}, \quad (\text{E5})$$

a degree-1 polynomial in i_O , identifying the output as $|T\rangle^{\otimes 4}$ up to Clifford correction. \checkmark

Appendix F: Asymmetric search: methods and catalogue

1. Search procedure

The asymmetric search enumerates over the skip parameters (s_{total}, s_O) with $s_S = 1$ fixed. For each parameter tuple $(l, n, k, s_{\text{total}}, s_O)$, the gate set \mathcal{W} is determined by the three weight-separation sets $\mathcal{W}_{\text{total}}, \mathcal{W}_O, \mathcal{W}_S$ as

described for asymmetric circuits. Validity is checked by verifying Eq. (7) at each Dicke sector (i_O, i_S) , with $\Phi(i_O, i_S)$ evaluated via Lemma 4 in $O(k(n-k))$ phase computations per sign assignment.

a. Sign assignment. At each parameter tuple, two deterministic sign assignments are checked in sequence. Cell 1 sets $\sigma_{w_O, w_S} = +1$ for every gate type. Cell 2 sets $\sigma_{0, w_S} = -1$ on every check-only gate type ($w_O = 0$) and $\sigma_{w_O, w_S} = +1$ on every gate touching at least one output qubit ($w_O \geq 1$). The parameter tuple is valid if Eq. (7) holds for either cell and invalid otherwise. Empirically, mixed sign patterns on check-only gates are never required to recover the factories listed in Tables I–III, so the sign-enumeration cost is bounded by 2 verifications per tuple rather than $2^{|W|}$. We check only whether one of the two cells succeeds, because under the two-group symmetry considered here, with $s_S = 1$, the sign assignment affects only validity and not the depth of the circuit. However, circuits with $s_S \neq 1$ or different permutation symmetries may yield more efficient factories from a search over mixed-sign types—this scope is left for future work.

b. Output classification. After extraction via Eq. (8), the residual phase polynomial $\Phi'(i_O, 0)/\theta$ is computed by finite differences in i_O . A polynomial of degree 1 in i_O corresponds to unentangled $|T\rangle^{\otimes k}$ outputs; a polynomial of degree 2, 3, \dots , l indicates an entangled \mathbb{C}_l magic state, with degree-2 giving $|\text{CS}\rangle$, degree-3 giving $|\text{CCZ}\rangle$, and degree- l at $l \geq 4$ giving the C^{l-1}Z gate of the l -th level. Solutions whose extracted output has vanishing residual phase are excluded as trivial stabilizer-state outputs. The rest are classified by residual polynomial degree (see App. D); for example, $[[8, 4, 2]]$ at $l = 3$ is CCZ-equivalent despite its four-qubit output and is classified as such in Fig. 1.

2. Search complexity and runtime

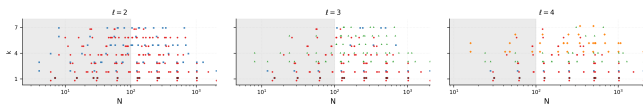


FIG. 2. Full extent of the two-group catalogue (N up to $\sim 10^3$); the shaded band marks the $N \leq 100$ region shown in Fig. 1.

For each (l, n, k) triple, the number of (s_{total}, s_O) parameter tuples is $|S_{\text{total}}| \times |S_O|$; per tuple, the deterministic two-cell check requires at most 2 verifications. Each verification costs $O(k(n-k))$ phase computations. The total cost at given (l, n, k) is thus

$$O(|S_{\text{total}}| \cdot |S_O| \cdot k(n-k)), \quad (\text{F1})$$

polynomial in n and k at fixed $|S_{\text{total}}|, |S_O|$.

To make this scaling concrete, we ran four sweeps of progressively wider parameter envelope: an $l \in \{2, 3\}, k \leq 4, n \leq 9, s_{\text{total}}, s_O \leq 4$ proof-of-concept range completes in 1.1 seconds; extending to $l \in \{2, 3, 4\}$ with the same other bounds gives 1.3 seconds; widening to $l \in \{2, 3, 4\}, k \leq 7, n \leq 11, s_{\text{total}}, s_O \leq 6$ takes ~ 7 seconds; and the full sweep used throughout this paper, $l \in \{2, 3, 4\}, k \leq 7, n \leq 11, s_{\text{total}}, s_O \leq 7$, completes in ~ 9 seconds on a standard laptop (Apple M4, 16 GB RAM) and produces 21,920 valid factories.

The sub-linear growth from ~ 7 to ~ 9 seconds across the $s_{\text{total}}, s_O \in \{1, \dots, 6\} \rightarrow \{1, \dots, 7\}$ extension reflects the early-termination structure: at fixed (l, n, k) , larger skip parameters admit progressively fewer gate types, so the verification at $(s_{\text{total}}, s_O) = (7, 7)$ is cheaper than at $(1, 1)$. The parameter range was chosen to cover all known distance-2 factories rather than to saturate the verifier; extending to larger n , larger k , or higher l carries trivial additional cost.

3. Catalogue of factory families

Tables I, II, and III list one representative per $(k, d, \text{output type, entanglement})$ combination recovered by the asymmetric search, at $l = 2, 3, 4$ respectively. Each row shows the smallest N realizing that combination, the smallest- n parameter tuple producing that N , and the output magic-state type. The full 21,920-entry catalogue, including all members of each family at every $n \leq 11$, is provided in the accompanying code repository [39].

a. Coverage relative to known catalogues. The Bravyi–Haah family $[[3k + 8, k, 2]]$ for $k = 2, 4, 6$ appears systematically at $(s_{\text{total}}, s_O) = (2, 2j - 1)$ with $k = 2j$: $[[14, 2, 2]]$ and $[[26, 6, 2]]$ are recovered with all-positive signs; $[[20, 4, 2]]$ requires negative signs $\sigma_{0,1} = \sigma_{0,3} = -1$ on the check-only gates, while the $k = 2$ and $k = 6$ members are not. The cube factory $[[8, 3, 2]]$ and the entangled-output factory $[[12, 2, 2]]$ are recovered with all-positive signs at $(s_{\text{total}}, s_O) = (1, 1)$. The Reed–Muller chain at $k = 1$ is recovered for $d \in \{2, 3\}$ via $s_{\text{total}} \in \{1, 2\}$. The extended sweep additionally captures every distance-2 entry of the Nezami–Haah triorthogonal-code catalogue [26] at the largest k for each $N \leq 32$.

b. New factory families at $l = 4$. A family of C^3Z -output factories appears at $l = 4, k = 4$, all-positive signs, $(s_{\text{total}}, s_O) = (1, 1)$: $[[16, 4, 2]]$ at $n = 5$ extending through $[[48, 4, 2]]$, $[[112, 4, 2]]$, $[[240, 4, 2]]$, $[[496, 4, 2]]$, $[[1008, 4, 2]]$, and $[[2032, 4, 2]]$ at $n = 11$. The smallest member, $[[16, 4, 2]]$, is the $l = 4$ analogue of the cube $[[8, 3, 2]]$ at $l = 3$: in both cases, a parent borrowed identity at $n = l + 2$ produces a degree- l output polynomial, the highest non-trivial \mathbb{C}_l magic state. Larger C^3Z -output families also appear at $k = 5, 6, 7$ within the swept range; see Table III.

TABLE I. Distance-2 family seeds at $l = 2$ recovered by the asymmetric search (for range covered in Fig. 1), limited to $N \leq 30$. The $k = 1$ rows with $s_{\text{total}} \geq 2$ (e.g. $[[7, 1]]$, $[[15, 1]]$) are distance-3; all other rows are distance-2.

$[[N, k]]$	class	n	s_{total}	s_O
$[[6, 1]]$	S	3	1	1
$[[7, 1]]$	S	4	2	1
$[[14, 1]]$	S	4	1	1
$[[15, 1]]$	S	5	2	1
$[[27, 1]]$	S	7	4	1
$[[30, 1]]$	S	5	1	1
$[[4, 2]]$	CZ	3	1	1
$[[6, 2]]$	S	4	2	1
$[[12, 2]]$	CZ	4	1	1
$[[14, 2]]$	S	5	2	1
$[[21, 2]]$	S	5	1	2
$[[22, 2]]$	S	6	2	2
$[[26, 2]]$	S	7	4	1
$[[28, 2]]$	CZ	5	1	1
$[[30, 2]]$	S	6	2	1
$[[4, 3]]$	CZ	4	2	1
$[[12, 3]]$	S	5	1	3
$[[12, 3]]$	CZ	5	2	1
$[[13, 3]]$	S	6	2	3
$[[25, 3]]$	S	7	4	1
$[[28, 3]]$	S	6	1	3
$[[28, 3]]$	CZ	6	2	1
$[[29, 3]]$	S	7	2	3
$[[6, 4]]$	CZ	5	1	3
$[[8, 4]]$	S	6	2	3
$[[18, 4]]$	CZ	6	1	3
$[[20, 4]]$	S	7	2	3
$[[24, 4]]$	S	7	4	1
$[[18, 5]]$	S	7	1	5
$[[19, 5]]$	S	8	2	5
$[[22, 5]]$	CZ	7	4	1
$[[8, 6]]$	CZ	7	1	5
$[[10, 6]]$	S	8	2	5
$[[16, 6]]$	S	7	4	1
$[[24, 6]]$	CZ	8	1	5
$[[26, 6]]$	S	9	2	5

TABLE II. Distance-2 family seeds at $l = 3$ recovered by the asymmetric search (for range covered in Fig. 1), limited to $N \leq 30$. The $k = 1$ row $[[15, 1]]$ ($s_{\text{total}} = 2$) is distance-3; all other rows are distance-2. Format as in Table I.

$[[N, k]]$	class	n	s_{total}	s_O
$[[14, 1]]$	T	4	1	1
$[[15, 1]]$	T	5	2	1
$[[30, 1]]$	T	5	1	1
$[[12, 2]]$	CS	4	1	1
$[[14, 2]]$	T	5	2	1
$[[28, 2]]$	CS	5	1	1
$[[30, 2]]$	T	6	2	1
$[[8, 3]]$	CCZ	4	1	1
$[[12, 3]]$	CCZ	5	2	1
$[[24, 3]]$	CCZ	5	1	1
$[[28, 3]]$	T	6	1	3
$[[28, 3]]$	CCZ	6	2	1
$[[29, 3]]$	T	7	2	3
$[[8, 4]]$	CCZ	5	2	1
$[[18, 4]]$	CCZ	6	1	3
$[[20, 4]]$	T	7	2	3
$[[24, 4]]$	CCZ	6	2	1
$[[24, 6]]$	CCZ	8	1	5
$[[26, 6]]$	T	9	2	5

TABLE III. Family seeds at $l = 4$ recovered by the asymmetric search (for range covered in Fig. 1), limited to $N \leq 30$. The C^3Z -output factories correspond to the new $l = 4$ family. Format as in Table I.

$[[N, k]]$	class	n	s_{total}	s_O
$[[30, 1]]$	\sqrt{T}	5	1	1
$[[28, 2]]$	CT	5	1	1
$[[30, 2]]$	\sqrt{T}	6	2	1
$[[24, 3]]$	CCS	5	1	1
$[[28, 3]]$	CCS	6	2	1
$[[16, 4]]$	$CCCZ$	5	1	1
$[[24, 4]]$	CCS	6	2	1
$[[16, 5]]$	$CCCZ$	6	2	1

Appendix G: Sequential search: methods and catalogue

c. Efficiency landmarks. Among small distance-2 factories with unentangled T output at $l = 3$, the $[[20, 4, 2]]$ Bravyi–Haah $k = 4$ factory attains $\gamma = \log_2(N/k) = \log_2(20/4) \approx 2.32$, second only to the Bravyi–Haah $k = 6$ factory $[[26, 6, 2]]$ ($\gamma \approx 2.12$) and tying with the catalytic factory $[[10, 2, 2]]$ ($\gamma \approx 2.32$ but with the smallest N) in the search-recovered set. For entangled CCZ -output factories, $[[8, 3, 2]]$ at $l = 3$ attains $\gamma = \log_2(8/3) = 1.4$, the smallest γ in the CCZ -output catalogue.

We can formalize the malleable circuits as follows. For each step $j \in \{1, 2, \dots\}$, the j th qubit is disentangled from the rest of the circuit using only multi-weight phase rotations. To do so, we construct a borrowed identity on the remaining $n - j$ qubits and extend each of its gates to also act on the j th qubit. After this circuit, the check qubit returns to $|+\rangle$ and is measured; what survives is an entangled magic state factory on $k = n - j$ qubits. In the main text, we have only discussed examples where s_j is the same for all steps j . Note that this is not a necessary condition, and we cover the general case of arbitrary s_j

in a brute-force search over sequential factories. Here, we give the closed-form disentangling condition for the sequential search with different s_j in each step.

1. Construction and phase condition

Definition 9 (Sequential borrowed identity). Let $\theta = \pi/2^l$ and partition n qubits into check qubits $\mathcal{S} = \{q_1, \dots, q_{n-k}\}$ and output qubits $\mathcal{O} = \{q_{n-k+1}, \dots, q_n\}$. A *sequential borrowed identity* is constructed by fixing each q_j in turn and applying all multi-weight phase rotation (Eq. 2) from $\{q_j, \dots, q_n\}$ with support containing q_j and weights in \mathcal{W}_j , until q_j returns to $|+\rangle$. The borrowed-identity gate count is

$$N = \sum_{j=1}^{n-k} \sum_{\substack{w \in \mathcal{W}_j \\ w \leq n-j+1}} \binom{n-j}{w-1}. \quad (\text{G1})$$

The output qubits are left in a k -qubit magic state $|\Psi_k\rangle$ for some diagonal \mathbb{C}_l gate [27], with the specific gate determined by the residual phase polynomial (App. D).

At step j , the active qubit q_j is in superposition $|0\rangle_j + e^{i\Delta\Phi_j(i)}|1\rangle_j$ entangled with Dicke states $|i\rangle$ over the remaining qubits. To disentangle q_j , we require $\Delta\Phi_j(i)$ to be (i) constant in i and (ii) an integer multiple of $\pi/2$, so that the residual qubit is a stabilizer state measurable as a check qubit.

Theorem 10 (Sequential phase condition). *For a sequential borrowed identity in which each Dicke-sector yields a local phase that is a multiple of 2π on the active qubit, the disentangling condition at step j is*

$$\Delta\Phi_j(i) = \begin{cases} 2^{i+1}\theta\sigma_j \sum_{w \in \mathcal{W}_j} \binom{n-j-i}{w-i}, & i \geq 1, j = 1, \\ 2\theta\sigma_j \sum_{w \in \mathcal{W}_j} \binom{n-j}{w-1} \\ + 2\theta \sum_{q=1}^{j-1} \sigma_q \sum_{w \in \mathcal{W}_q} \binom{n-q-1}{w-1}, & i = 0, \\ 0, & i \geq 1, j > 1, \end{cases} \quad (\text{G2})$$

where all cases are taken mod 2π and $\sigma_j \in \{\pm 1\}$ are per-step signs. For $j = 1$ this recovers Theorem 3. Generically, the construction terminates at $j_f = l$, when the residual phase prefactor reaches 2θ and the output qubits encode a \mathbb{C}_l magic state.

The three cases reflect the structure of the phase accumulation. For $j = 1$ and $i \geq 1$, the standard Dicke-sector simplification of the even-odd parity difference applies directly. For $j > 1$ and $i > 0$, the even and odd parity sums of the local gate contribution cancel identically, and the residual contributions from earlier steps also cancel

mod 2π , giving $\Delta\Phi_j(i) = 0$. For $i = 0$, the odd parity sum vanishes (no odd $m \leq 0$), so only the even parity sum contributes to the local phase; likewise $\Phi(0, j-1, 0) = 0$ for the same reason, so the residual reduces to $\Phi(1, j-1, 0)$, giving the cumulative expression in Eq. (G2). Each sequence step halves the residual phase prefactor, so after step j every nonzero Dicke sector carries a phase $2^{l+1-j}\theta$, equal to 2θ at $j = l$.

2. Worked examples

We verify Eq. (G2) explicitly for the four- and five-qubit malleable parent circuits discussed in the main text, working at $l = 3$ ($\theta = \pi/8$, $2\pi/\theta = 16$) with skip parameter $s = 1$ unless otherwise stated. The four-qubit parent ($n = 4$, $\mathcal{W}_j = \{1, \dots, n-j+1\}$) produces a sequential chain $[[8, 3, 2]] \rightarrow [[12, 2, 2]] \rightarrow [[14, 1, 2]]$, and the five-qubit parent ($n = 5$, $s = 2$, odd weights $\mathcal{W}_j = \{w \leq n-j+1 : w \text{ odd}\}$) extends this to $[[8, 4, 2]] \rightarrow [[12, 3, 2]] \rightarrow [[14, 2, 2]] \rightarrow [[15, 1, 3]]$.

a. *Step $j = 1$: $[[8, 3, 2]]$ and $[[8, 4, 2]]$.* For $\mathcal{W}_1 = \{1, 2, 3, 4\}$ at $n = 4$, the $i \geq 1$ condition gives

$$\Delta\Phi_1(i)/\theta = 2^{i+1} \sum_{w=1}^4 \binom{3-i}{w-i} = 2^{i+1} \cdot 2^{3-i} = 16 \equiv 0,$$

and at $i = 0$: $2 \sum_w \binom{3}{w-1} = 2 \cdot 8 = 16 \equiv 0$. This yields $[[8, 3, 2]]$ (QUIRK) with output $|\text{CCZ}\rangle$ (App. E 1). At $n = 5$ with $s = 2$, $\mathcal{W}_1 = \{1, 3, 5\}$: $2 \sum_{w \in \mathcal{W}_1} \binom{4}{w-1} = 2(1+6+1) = 16 \equiv 0$ and $2^{i+1} \sum_{w \in \mathcal{W}_1} \binom{4-i}{w-i} \equiv 0$ for $i \geq 1$, yielding $[[8, 4, 2]]$ (QUIRK) with output Clifford-equivalent to $|\text{CCZ}\rangle$.

b. *Step $j = 2$: $[[12, 2, 2]]$ and $[[12, 3, 2]]$.* At $n = 4$, adding $\mathcal{W}_2 = \{1, 2, 3\}$:

$$\begin{aligned} \Delta\Phi_2(0)/\theta &= 2 \sum_{w \in \mathcal{W}_2} \binom{2}{w-1} + 2 \sum_{w \in \mathcal{W}_1} \binom{2}{w-1} \\ &= 2(1+2+1) + 2(1+2+1+0) = 16 \equiv 0, \end{aligned}$$

yielding $[[12, 2, 2]]$ (QUIRK) with output $|\text{CS}\rangle$. At $n = 5$ with $s = 2$ ($\mathcal{W}_1 = \{1, 3, 5\}$, $\mathcal{W}_2 = \{1, 3\}$):

$$\begin{aligned} \Delta\Phi_2(0)/\theta &= 2 \sum_{w \in \mathcal{W}_2} \binom{3}{w-1} + 2 \sum_{w \in \mathcal{W}_1} \binom{3}{w-1} \\ &= 8 + 8 = 16 \equiv 0, \end{aligned}$$

yielding $[[12, 3, 2]]$ (QUIRK) with output Clifford-equivalent to $|\text{CCZ}\rangle$.

c. *Step* $j = 3$: $[[14, 1, 2]]$ and $[[14, 2, 2]]$. At $n = 4$, adding $\mathcal{W}_3 = \{1, 2\}$:

$$\begin{aligned} \Delta\Phi_3(0)/\theta &= 2 \sum_{w \in \mathcal{W}_3} \binom{1}{w-1} + 2 \sum_{w \in \mathcal{W}_2} \binom{1}{w-1} \\ &\quad + 2 \sum_{w \in \mathcal{W}_1} \binom{2}{w-1} \\ &= 2(1+1) + 2(1+1+0) + 2(1+2+1+0) \\ &= 16 \equiv 0, \end{aligned}$$

yielding $[[14, 1, 2]]$ (QUIRK) with output $|T\rangle$. At $n = 5$ with $s = 2$, $\mathcal{W}_1 = \{1, 3, 5\}$, $\mathcal{W}_2 = \mathcal{W}_3 = \{1, 3\}$:

$$\begin{aligned} \Delta\Phi_3(0)/\theta &= 2 \sum_{w \in \mathcal{W}_3} \binom{2}{w-1} + 2 \sum_{w \in \mathcal{W}_2} \binom{2}{w-1} \\ &\quad + 2 \sum_{w \in \mathcal{W}_1} \binom{3}{w-1} \\ &= 4 + 4 + 8 = 16 \equiv 0, \end{aligned}$$

yielding $[[14, 2, 2]]$ (QUIRK) with output $|T\rangle$ at distance 2.

d. *Step* $j = 4$: $[[15, 1, 3]]$. At $n = 5$ with $s = 2$, adding $\mathcal{W}_4 = \{1\}$:

$$\begin{aligned} \Delta\Phi_4(0)/\theta &= 2 \sum_{w \in \mathcal{W}_4} \binom{1}{w-1} + 2 \sum_{w \in \mathcal{W}_3} \binom{1}{w-1} \\ &\quad + 2 \sum_{w \in \mathcal{W}_2} \binom{2}{w-1} + 2 \sum_{w \in \mathcal{W}_1} \binom{3}{w-1} \\ &= 2 + 2 + 4 + 8 = 16 \equiv 0, \end{aligned}$$

yielding $[[15, 1, 3]]$ (QUIRK) with output $|T\rangle$ at distance 3, completing the five-qubit parent chain.

e. *Catalytic conversions*. Applying a Clifford+ T catalytic $|\text{CCZ}\rangle \rightarrow |T\rangle$ conversion to the $j = 1$ output of the four-qubit parent yields $[[11, 1, 2]]$ (QUIRK) when one output qubit is retained, and $[[10, 2, 2]]$ (QUIRK) when two are retained. Both are verified for the teleported- T case, accounting for Z - and S -type errors on the conversion ancilla.

3. Results and qualitative features

The sequential search results are shown in Fig. 3. For each (l, n) with $l \in \{2, 3, 4\}$ and $n \leq 6$, we enumerate sequences $(\mathcal{W}_1, \dots, \mathcal{W}_J)$ with $J = n - k$ and each $\mathcal{W}_j = \{w \equiv 1 \pmod{s_j} : w \leq n - j + 1\}$ for $s_j \in \{1, 2, 3, 4\}$, giving 4^J candidate tuples per (n, J) . Each candidate is verified in $O(J^2 n)$ time by evaluating Eq. (G2) for all i at every step. The full search to $n = 6$ completes in well under one second.

a. *Non-monotonicity in l* . Unlike the symmetric case, the sequential condition is *not* a monotone in l : the prefactor $2^{i+1}\theta$ depends on l through $\theta = \pi/2^l$ in a way

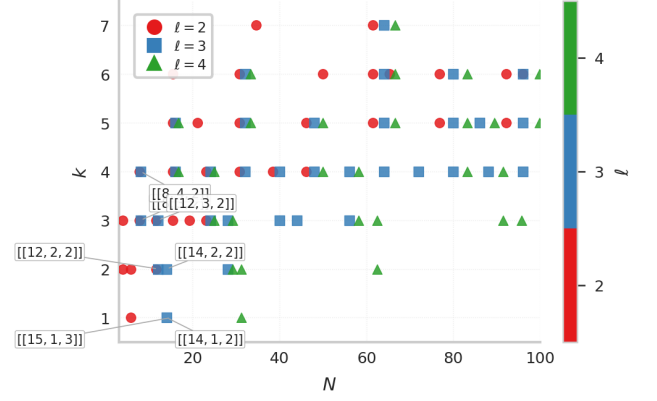


FIG. 3. **Sequential distillation factories.** Each marker shows a factory at coordinate (N, k) ; color and shape both encode the Clifford-hierarchy level l (red circles: $l = 2$; blue squares: $l = 3$; green triangles: $l = 4$). We have restricted the search to $j_{\max} = l$. Multiple markers at the same coordinate indicate factories valid at multiple l via independent solutions of Theorem 10. See Table IV for full enumeration of sequential search output not found in the asymmetric search.

TABLE IV. All non-trivial distance-2 sequential search outputs with $l \in \{2, 3, 4\}$, $n \leq 6$, $j_{\max} = l$ that are not found by the asymmetric search. For each (l, N, k) : smallest n admitting a solution and lexicographically smallest per-step skip tuple $\mathbf{s} = (s_1, \dots, s_{n-k})$ satisfying Theorem 10 with all $\sigma_j = +1$.

N	k	n	\mathbf{s}	1
16	3	5	(2, 1)	2
20	3	5	(1, 2)	2
40	4	6	(1, 2)	2
32	5	6	(1)	2
40	3	6	(2, 1, 1)	3
44	3	6	(1, 2, 2)	3
40	4	6	(1, 2)	3
32	5	6	(1)	3
32	5	6	(1)	4

that does not factor through $l \rightarrow l - 1$. A sequence $(\mathcal{W}_1, \dots, \mathcal{W}_J)$ that disentangles at one l generically does not disentangle for all $l' < l$. Thus, solutions at different l are independent.

b. *Sign redundancy*. Each step j carries a sign $\sigma_j \in \{+1, -1\}$. Exhaustive search over both branches shows that sign flips relabel solutions without producing new code parameters; the sign tuple is suppressed in Table IV.

Appendix H: Symmetry-free targeted search on extended borrowed identities for synthillation circuits

We extend the borrowed identity formalism to include multi-weight phase rotations by angle $c\pi/2^i$ where $i \leq l$ and $c \in \mathbb{Z}_{2^i}$. The extended borrowed-identity condi-

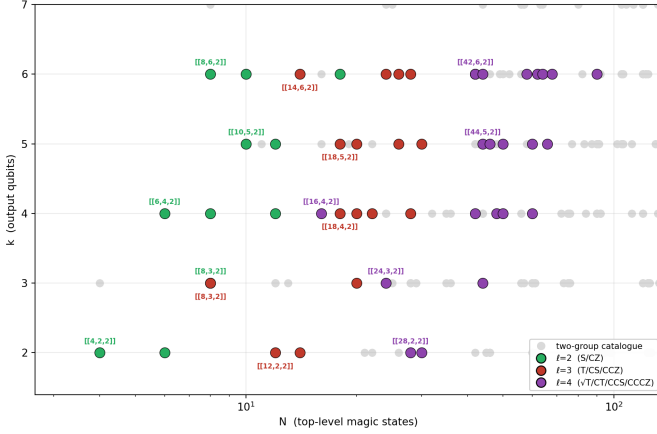


FIG. 4. Factories from the symmetry-free targeted-output search (colored) over the two-group symmetric catalogue (gray), at $l = 2, 3, 4$, in the (N, k) plane ($N =$ top-level magic states, $k =$ output qubits). The minimal- N factory at each k is labeled by $[[N, k, d]]$ and its block composition.

tion (1) is *linear* over $\mathbb{Z}_{2^{l+1}}$ in the gate coefficients $\{c\}$. This makes a direct, symmetry-free search possible: instead of restricting the gate set to a symmetric weight-class ansatz, we fix a *target output* and *solve* for the rest of the circuit. For a chosen output structure—a partition of the k output qubits into magic blocks—the output gates are fixed and the borrowed-identity condition is solved for the remaining check-coupling gates by 2-adic Gaussian elimination, taking the smallest check register that admits a solution.

Re-expressed at the common scale $\pi/2^l$, the coefficients are unconstrained ($c \in \mathbb{Z}_{2^{l+1}}$), so the solver freely places lower-level (Clifford) rotations. This extension of the borrowed identity is suited to synthillation circuits, which admit all diagonal gates of Clifford-hierarchy level \mathcal{C}_l together with the lower levels $\mathcal{C}_{l' < l} \subset \mathcal{C}_l$ [27]. We re-

port N as the number of top-level ($\pi/2^l$, odd-coefficient) magic gates—Clifford gates being free—and compute the distance over these. The construction is *exact* (a linear solve, not heuristic enumeration); but the final reduction of N is greedy. Figure 4 shows the factories found by this symmetry-free search at $l = 2, 3, 4$ that lie outside the two-group symmetric ansatz. They serve as an existence proof that synthillation circuits fall under the borrowed-identity framework with minimal changes.

This symmetry-free targeted-output search is fast but only complementary to the two-group symmetric search discussed in the main text. A symmetry-free SAT search based on our extended borrowed identity condition is inclusive of both and includes higher-distance factories, only excluding the non-CSS results like $[[10, 2, 2]]$. However, this search is too slow to achieve the final goal of finding the smallest $k > 1$ factories at all distances. This SAT search is also general over all Clifford levels.

Appendix I: Canonical examples

TABLE V. Canonical instances for borrowed-identity based distillation factories at level l of the Clifford hierarchy. Clickable links to interactive Quirk circuits [36] for some instances are provided.

Approach (§)	$l = 2$	$l = 3$	$l = 4$
Symmetric (all weights, § 0 a)	[[6, 1, 2]]	[[14, 1, 2]]	[[30, 1, 2]]
Symmetric (odd weights, § 0 a)	[[7, 1, 3]]	[[15, 1, 3]]	[[31, 1, 3]]
Two-group (deg= 1, § 0 b)	[[6, 2, 2]]	[[14, 2, 2]]	[[30, 2, 2]]
Two-group (deg= 1, § 0 b)	[[8, 4, 2]]	[[20, 4, 2]]	[[44, 4, 2]]
Two-group (deg= 1, § 0 b)	[[10, 6, 2]]	[[26, 6, 2]]	[[58, 6, 2]]
Two-group (deg= 2, § 0 b)	[[4, 2, 2]]	[[12, 2, 2]]	[[28, 2, 2]]
Two-group (deg= 3, § 0 b)	–	[[8, 3, 2]]	[[24, 3, 2]]
Two-group (deg= 3, § 0 b)	–	[[24, 6, 2]]	[[403, 6, 2]]
Two-group (deg= 4, § 0 b)	–	–	[[16, 4, 2]]
Catalytic (§ 0 c)	–	[[11, 1, 2]]	–
Catalytic (§ 0 c)	–	[[10, 2, 2]]	–

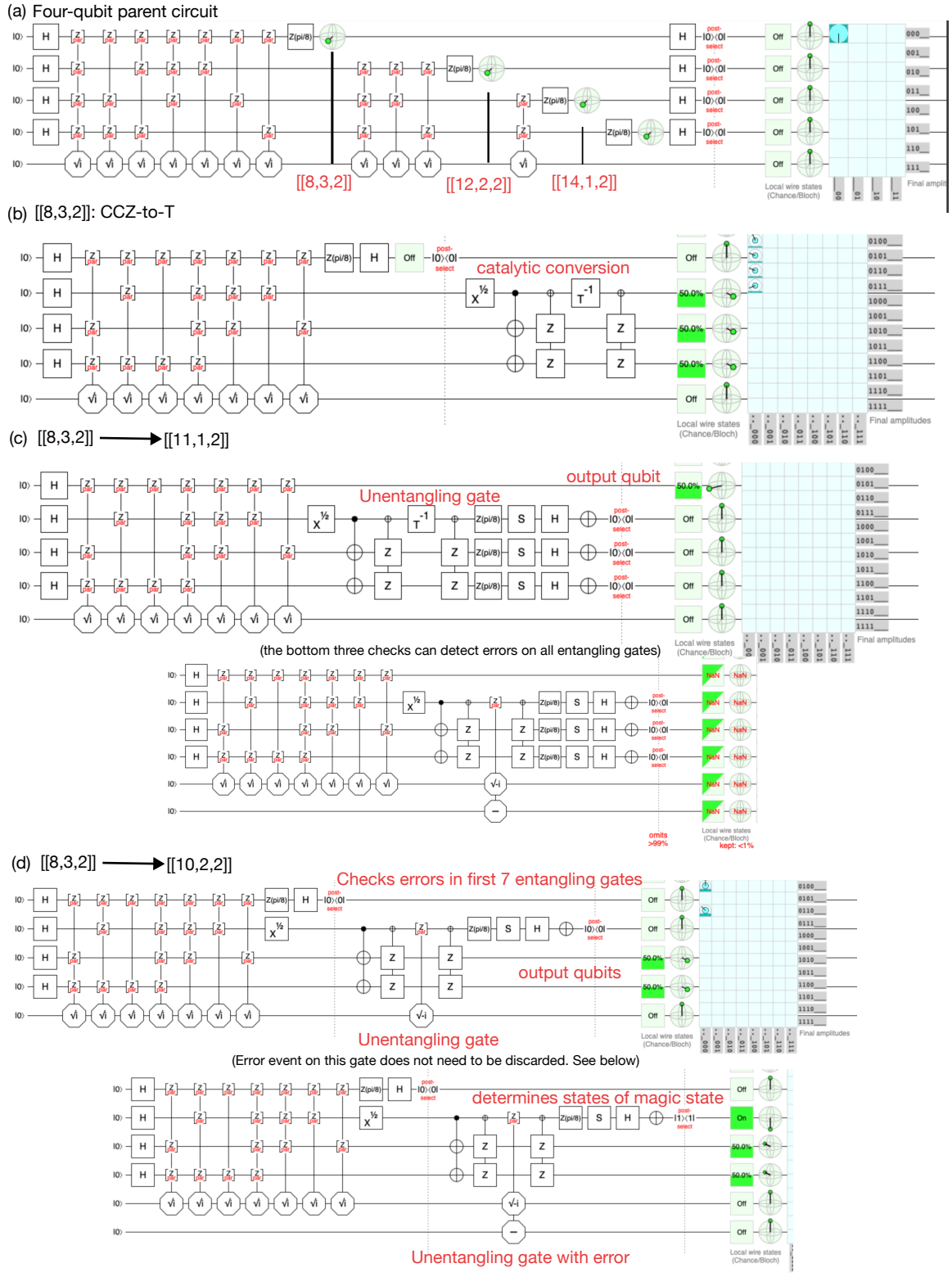
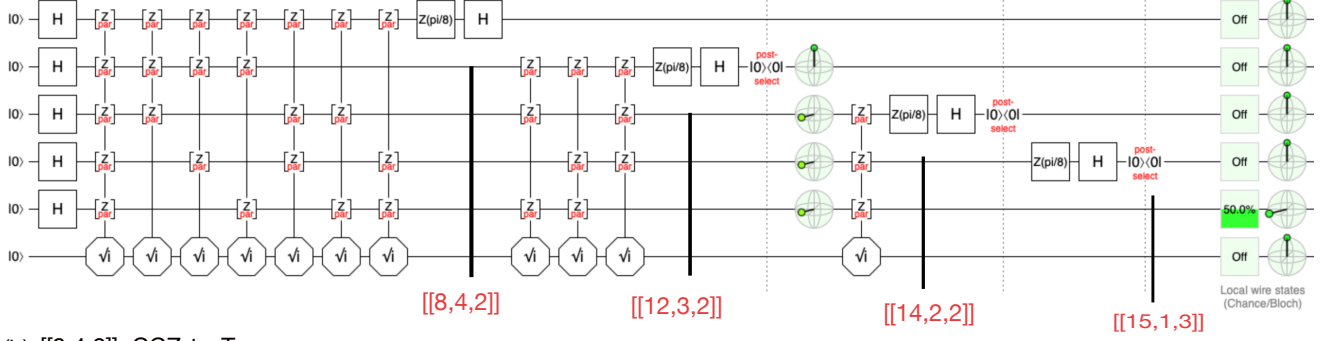
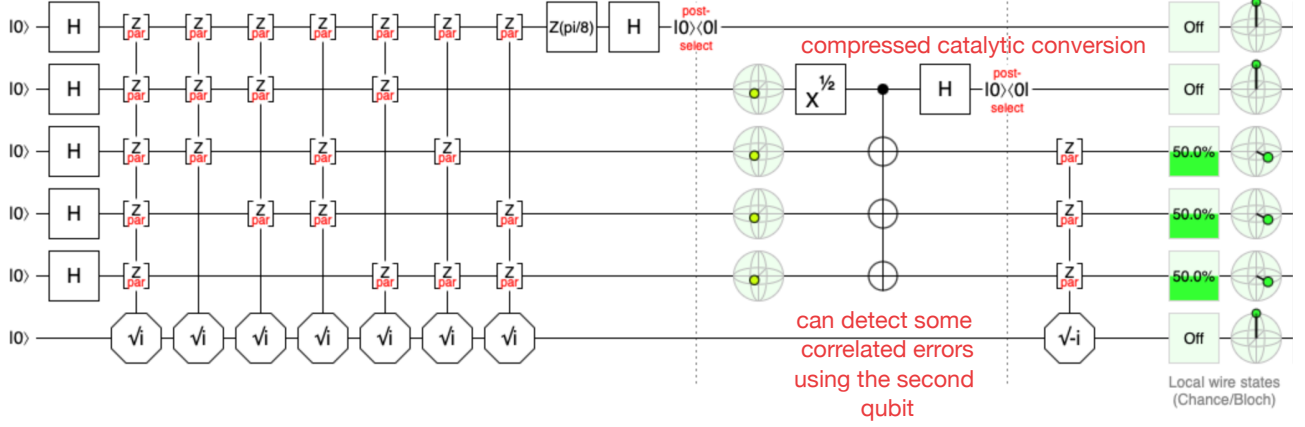


FIG. 5. **The four-qubit parent circuit** [LINK]. The conditional \sqrt{i} denotes multi-weight $\pi/8$ rotations [18, 36]. (a) The malleable circuit showing $[[8, 3, 2]] \rightarrow [[12, 2, 2]] \rightarrow [[14, 1, 2]]$. Note that the T -to- CS factory $[[12, 2, 2]]$ (equivalent to the $4 CS \rightarrow 1 CS$) is *larger* than the T -to- CCZ factory $[[8, 3, 2]]$, even though CS is a lower-level gate, because the number of gates removed from the identity equals the number of T states the output consumes in its unitary synthesis—3 for CS versus 7 for CCZ . Another reason for this is that any pure T -to- CS distance-2 factory which cannot be interpreted as CS -to- CS circuit (analogous to $[[8, 3, 2]]$) requires a borrowed identity on 3 qubits which is not possible for $l = 3$ (see Sec. 0a). (b) The three-qubit circuit from the $[[8, 3, 2]]$ circuit obeys the catalytic CCZ -to- T conversion. (c) The catalytic conversion to the $[[11, 1, 2]]$ circuit (top qubit is the output) [LINK]. (d) The catalytic conversion to the $[[10, 2, 2]]$ circuit [LINK], where the error on the unentangling gate does not need to be discarded. The canonical instance of each construction at every level l is collected in Table V.

(a) Five-qubit parent circuit

(b) $[[8,4,2]]$: CCZ-to-T

(c) Six-qubit parent circuit

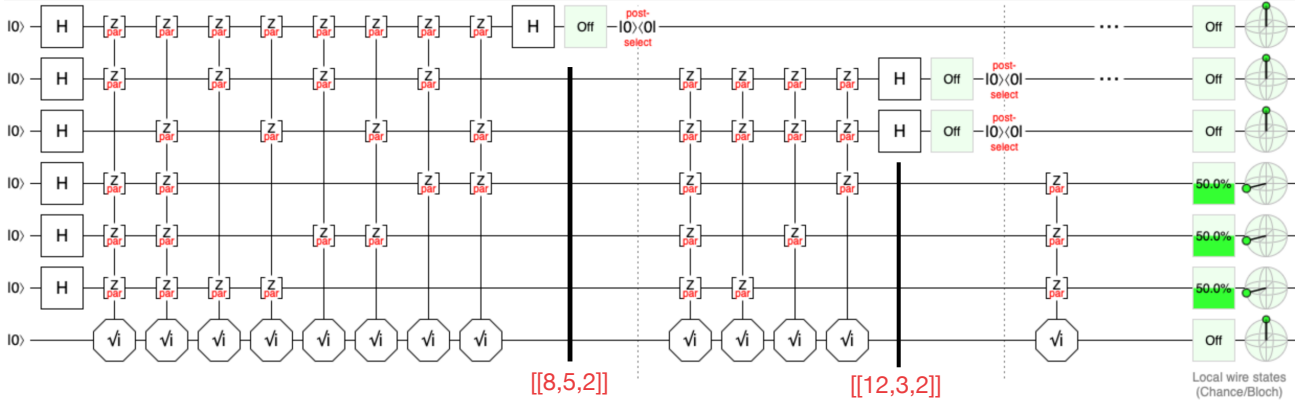


FIG. 6. **The five-qubit $[[LINK]]$ and six-qubit $[[LINK]]$ parent circuits.** The conditional \sqrt{i} denotes multi-weight $\pi/8$ rotations [18, 36]. (a) The malleable circuit showing $[[8, 4, 2]] \rightarrow [[12, 3, 2]] \rightarrow [[14, 2, 2]]$. By reducing the output to one qubit, this becomes an example of $s = 2$ (see Section 0a), yielding distance-3 factory $[[15, 1, 3]]$. Note that the $[[12, 3, 2]]$ factory output also requires only one ‘catalytic’ T rotation to un-entangle the outputs into 3 T states. Therefore, the $[[12, 3, 2]]$ output is also CCZ-equivalent. (b) The four-qubit output from the $[[8, 4, 2]]$ is Clifford equivalent to a CCZ state, yielding 3 T states via catalytic conversion. This four-qubit output can detect some correlated errors which flip the $X \otimes X \otimes X$ measurement. (c) The extension to a six-qubit parent factory yields a 5-qubit output Clifford-equivalent to the CCZ state.